

# Large volumetric thermal expansion of a novel organic cocrystal over a wide temperature range

Lukman O. Alimi, Prem Lama, Vincent J. Smith and Leonard J. Barbour\*

Department of Chemistry and Polymer Science, University of Stellenbosch, Matieland 7602, South Africa.

E-mail: [ljb@sun.ac.za](mailto:ljb@sun.ac.za)

## Supplementary Information:

- 1) Experimental Information:**
- 2) Single crystal X-ray diffraction measurements**
- 3) Unit cell parameters for ABN·2DMABN cocrystal from 300 to 100 K at 20 K intervals**
- 4) Powder X-ray diffraction measurements**
- 5) Hot stage Microscopy**
- 6) Differential Scanning Calorimetry**
- 7) Thermal expansion coefficients**
- 8) Intermolecular interactions within the structure**

## 1) Experimental Information

The 4-aminobenzonitrile (ABN) and 4-(dimethylamino)benzonitrile (DMABN) used in the preparation of **ABN·2DMABN** cocrystal were purchased from Sigma Aldrich and used without further purification.

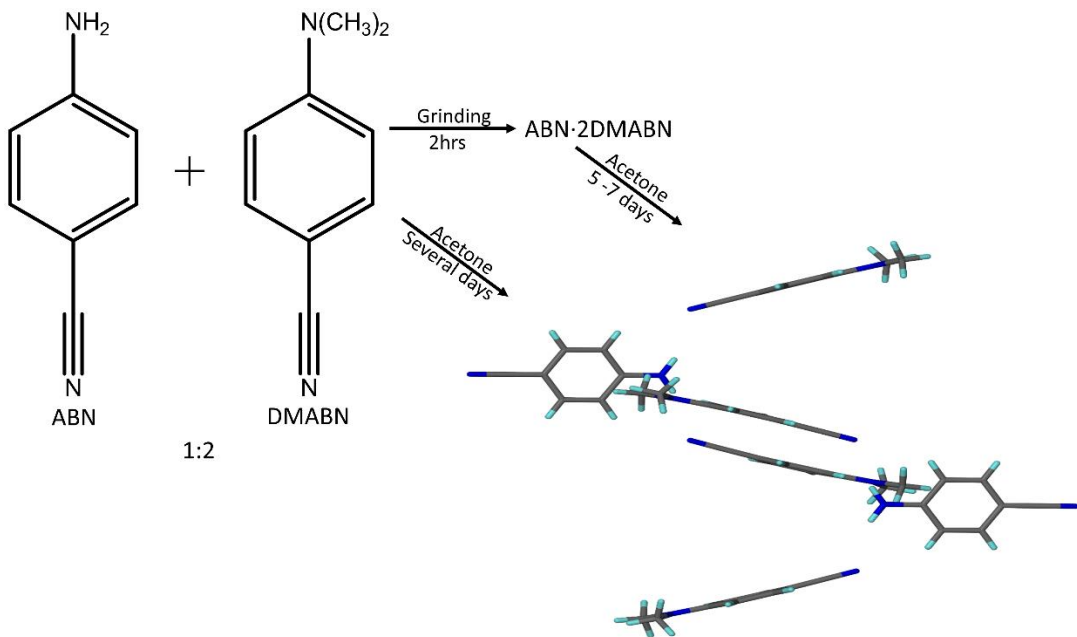
### Preparation of ABN·2DMABN cocrystal:

#### Method 1

Cocrystals were obtained by dissolving ABN (59.07 mg, 0.5 mmol) and DMABN (146.19 mg, 1.0 mmol) in 1ml of acetone. Slow evaporation over several days yielded single crystals suitable for X-ray diffraction.

#### Method 2

The mechanochemical method was also used for cocrystallisation. ABN (100 mg, 0.85 mmol) was ground with DMABN (248.5 mg, 1.7 mmol) in a pre-washed and dried agate mortar and pestle. The combination was ground for 2 h; the formation of the new materials was monitored by periodically measuring the PXRD pattern until a new pattern emerged. Cocrystals were obtained by dissolving (20 mg, 0.049 mmol) of ground materials in 1ml of acetone. Slow evaporation over 5-7 days yielded single crystals suitable for X-ray diffraction.



**Scheme S1:** Formation of the **ABN·2DMABN** cocrystal.

## 2) Single crystal X-ray diffraction measurements

Single-crystal X-ray diffraction data were collected using a Bruker APEX-II Quasar CCD area detector diffractometer equipped with an Oxford Cryosystems 700Plus cryostat. A multilayer monochromator with Mo K $\alpha$  radiation ( $\lambda = 0.71073 \text{ \AA}$ ) from an Incoatec I $\mu$ S micro source was used. Data reduction was carried out by means of a standard procedure using the Bruker software package SAINT.<sup>1</sup> Absorption corrections and correction of other systematic errors were performed using SADABS.<sup>2,3</sup> The structures were solved by direct methods using SHELXS-2016 and refined using SHELXL-2016.<sup>4</sup> X-Seed was used as the graphical interface for the SHELX program suite.<sup>5</sup> Hydrogen atoms were placed in calculated positions using riding models.

**Table S1.** Crystallographic details for **ABN·2DMABN** cocrystal

Identification code	ABN·2DMAB N_300 K	ABN·2DMAB N_280 K	ABN·2DMAB N_260 K	ABN·2DMAB N_240 K	ABN·2DMAB N_220 K	ABN·2DMAB N_200 K
Empirical formula	C <sub>25</sub> H <sub>26</sub> N <sub>6</sub>					
Formula weight/g/mol	410.52	410.52	410.52	410.52	410.52	410.52
Temperature/K	300(2)	280(2)	260(2)	240(2)	220(2)	200(2)
Crystal system	Monoclinic	Monoclinic	Monoclinic	Monoclinic	Monoclinic	Monoclinic
Space group	P2 <sub>1</sub> /n					
a/ $\text{\AA}$	9.8177(10)	9.8071(2)	9.7994(2)	9.7912(2)	9.7836(2)	9.7770(3)
b/ $\text{\AA}$	25.6597(31)	25.6011(7)	25.5488(7)	25.4967(8)	25.4438(8)	25.3964(10)
c/ $\text{\AA}$	19.3047(23)	19.2577(5)	19.2173(5)	19.1789(5)	19.1399(6)	19.1058(7)
$\alpha/^\circ$	90	90.00	90.00	90.00	90.00	90.00
$\beta/^\circ$	104.384(4)	104.347(1)	104.313(1)	104.291(1)	104.278(1)	104.272(1)
$\gamma/^\circ$	90	90.00	90.00	90.00	90.00	90.00
Volume/ $\text{\AA}^3$	4710.8(9)	4684.3(2)	4662.0(2)	4639.7(2)	4617.4(2)	4597.6(3)
Z	8	8	8	8	8	8
$\rho_{\text{calc}}/\text{cm}^3$	1.158	1.164	1.170	1.175	1.181	1.186
$\mu/\text{mm}^{-1}$	0.072	0.072	0.072	0.073	0.073	0.073
F(000)	1744	1744	1744	1744	1744	1744
Crystal size/mm <sup>3</sup>	0.335 × 0.242 × 0.116	0.334 × 0.241 × 0.115	0.333 × 0.24 × 0.114	0.332 × 0.239 × 0.113	0.331 × 0.238 × 0.112	0.33 × 0.237 × 0.111
Radiation	MoK $\alpha$ ( $\lambda = 0.71073$ )					
$\theta$ range for data collection/ $^\circ$	1.35 to 28.44	1.35 to 28.34	1.35 to 28.51	1.36 to 28.39	1.36 to 28.29	1.36 to 28.32
Index ranges	-13 ≤ h ≤ 11, -34 ≤ k ≤ 34, -25 ≤ l ≤ 25	-11 ≤ h ≤ 13, -34 ≤ k ≤ 34, -25 ≤ l ≤ 25	-11 ≤ h ≤ 13, -34 ≤ k ≤ 34, -25 ≤ l ≤ 25	-11 ≤ h ≤ 13, -34 ≤ k ≤ 34, -25 ≤ l ≤ 25	-11 ≤ h ≤ 13, -33 ≤ k ≤ 33, -25 ≤ l ≤ 25	-11 ≤ h ≤ 13, -33 ≤ k ≤ 33, -25 ≤ l ≤ 25
Reflections collected	166146	165295	163100	163738	162781	147347
Independent reflections	11782 [R <sub>int</sub> = 0.0759, R <sub>sigma</sub> = 0.0349]	11659 [R <sub>int</sub> = 0.0854, R <sub>sigma</sub> = 0.0394]	11736 [R <sub>int</sub> = 0.0836, R <sub>sigma</sub> = 0.0396]	11588 [R <sub>int</sub> = 0.0808, R <sub>sigma</sub> = 0.0384]	11444 [R <sub>int</sub> = 0.0788, R <sub>sigma</sub> = 0.0361]	11422 [R <sub>int</sub> = 0.0768, R <sub>sigma</sub> = 0.0374]
Data/restraints/parameters	11782/0/567	11659/0/567	11736/0/567	11588/0/567	11444/0/567	11422/0/567
Goodness-of-fit on F <sup>2</sup>	1.035	1.061	1.066	1.046	1.046	1.051
Final R indexes [ $I >= 2\sigma(I)$ ]	R <sub>1</sub> = 0.0727, wR <sub>2</sub> = 0.2049	R <sub>1</sub> = 0.0703, wR <sub>2</sub> = 0.1864	R <sub>1</sub> = 0.0683, wR <sub>2</sub> = 0.1839	R <sub>1</sub> = 0.0647, wR <sub>2</sub> = 0.1615	R <sub>1</sub> = 0.0639, wR <sub>2</sub> = 0.1606	R <sub>1</sub> = 0.0613, wR <sub>2</sub> = 0.1490
Final R indexes [all data]	R <sub>1</sub> = 0.1592, wR <sub>2</sub> = 0.2735	R <sub>1</sub> = 0.1653, wR <sub>2</sub> = 0.2595	R <sub>1</sub> = 0.1578, wR <sub>2</sub> = 0.2543	R <sub>1</sub> = 0.1472, wR <sub>2</sub> = 0.2279	R <sub>1</sub> = 0.1359, wR <sub>2</sub> = 0.2171	R <sub>1</sub> = 0.1337, wR <sub>2</sub> = 0.2041
Largest diff. peak/hole / e $\text{\AA}^{-3}$	0.14/-0.16	0.188/-0.191	0.17/-0.19	0.18/-0.22	0.18/-0.21	0.21/-0.21
Mosaicity	0.39	0.38	0.38	0.38	0.38	0.38
CCDC number	1555132	1555131	1555130	1555129	1555128	1555127

**Table S1.** Crystallographic details for **ABN·2DMABN** cocrystal continued.

Identification code	ABN·2DMABN_180 K	ABN·2DMABN_160 K	ABN·2DMABN_140 K	ABN·2DMABN_120 K	ABN·2DMABN_100 K
Empirical formula	C <sub>25</sub> H <sub>26</sub> N <sub>6</sub>				
Formula weight	410.52	410.52	410.52	410.52	410.52
Temperature/K	180(2)	160(2)	140(2)	120(2)	100(2)
Crystal system	Monoclinic	Monoclinic	Monoclinic	Monoclinic	Monoclinic
Space group	P2 <sub>1</sub> /n				
<i>a</i> /Å	9.7754(3)	9.7730(3)	9.7661(3)	9.7650(3)	9.7654(4)
<i>b</i> /Å	25.3489(8)	25.2982(8)	25.2392(8)	25.1863(9)	25.1269(11)
<i>c</i> /Å	19.0721(6)	19.0409(6)	19.0103(6)	18.9850(7)	18.9626(8)
$\alpha^{\circ}$	90.00	90.00	90.00	90.00	90.00
$\beta^{\circ}$	104.284(10)	104.279(1)	104.274(1)	104.254(1)	104.199 (1)
$\gamma^{\circ}$	90.00	90.00	90.00	90.00	90.00
Volume/Å <sup>3</sup>	4579.9(2)	4561.0(2)	4541.2(2)	4525.5(3)	4510.8(3)
<i>Z</i>	8	8	8	8	8
$\rho_{\text{calc}}/\text{g/cm}^3$	1.191	1.196	1.201	1.205	1.209
$\mu/\text{mm}^{-1}$	0.074	0.074	0.074	0.074	0.075
F(000)	1744.0	1744.0	1744.0	1744.0	1744.0
Crystal size/mm <sup>3</sup>	0.329 × 0.236 × 0.11	0.328 × 0.235 × 0.109	0.327 × 0.234 × 0.108	0.326 × 0.233 × 0.107	0.325 × 0.232 × 0.106
Radiation	MoKα ( $\lambda = 0.71073$ )				
θ range for data collection/°	1.61 to 28.37	2.66 to 28.35	138 to 28.36	1.37 to 28.38	1.37 to 28.34
Index ranges	-11 ≤ <i>h</i> ≤ 13, -33 ≤ <i>k</i> ≤ 33, -25 ≤ <i>l</i> ≤ 25	-11 ≤ <i>h</i> ≤ 13, -33 ≤ <i>k</i> ≤ 33, -25 ≤ <i>l</i> ≤ 25	-11 ≤ <i>h</i> ≤ 13, -33 ≤ <i>k</i> ≤ 33, -25 ≤ <i>l</i> ≤ 25	-11 ≤ <i>h</i> ≤ 13, -33 ≤ <i>k</i> ≤ 33, -25 ≤ <i>l</i> ≤ 25	-11 ≤ <i>h</i> ≤ 13, -33 ≤ <i>k</i> ≤ 33, -25 ≤ <i>l</i> ≤ 25
Reflections collected	211399	210216	209426	154099	178039
Independent reflections	11269 [R <sub>int</sub> = 0.0948, R <sub>sigma</sub> = 0.0359]	11218 [R <sub>int</sub> = 0.0952, R <sub>sigma</sub> = 0.0354]	11237 [R <sub>int</sub> = 0.0954, R <sub>sigma</sub> = 0.0352]	11236 [R <sub>int</sub> = 0.0909, R <sub>sigma</sub> = 0.0389]	11176 [R <sub>int</sub> = 0.0952, R <sub>sigma</sub> = 0.0379]
Data/restraints/parameters	11269/0/567	11218/0/567	11237/0/567	11236/0/567	11176/0/567
Goodness-of-fit on F <sup>2</sup>	1.026	1.020	1.037	1.026	1.033
Final R indexes [I>=2σ (I)]	R <sub>1</sub> = 0.0898, wR <sub>2</sub> = 0.2265	R <sub>1</sub> = 0.0953, wR <sub>2</sub> = 0.2229	R <sub>1</sub> = 0.0888, wR <sub>2</sub> = 0.2262	R <sub>1</sub> = 0.0876, wR <sub>2</sub> = 0.2192	R <sub>1</sub> = 0.0886, wR <sub>2</sub> = 0.2249
Final R indexes [all data]	R <sub>1</sub> = 0.1472, wR <sub>2</sub> = 0.3061	R <sub>1</sub> = 0.1425, wR <sub>2</sub> = 0.2958	R <sub>1</sub> = 0.1366, wR <sub>2</sub> = 0.2896	R <sub>1</sub> = 0.1383, wR <sub>2</sub> = 0.2858	R <sub>1</sub> = 0.1321, wR <sub>2</sub> = 0.2833
Largest diff. peak/hole / e Å <sup>-3</sup>	0.29/-0.36	0.29/-0.40	0.39/-0.42	0.34/-0.45	0.49/-0.48
Mosaicity	0.38	0.38	0.38	0.38	0.38
CCDC number	1555126	1555125	1555124	1555122	1555123

### 3) Unit cell parameters for ABN·2DMABN cocrystal from 300 to 100 K at 20 K intervals

**Table S2.** Unit cell axes and cell volume at variable temperatures for **ABN·2DMABN** Cocrystal

T (K)	<i>a</i> (Å)	St. dev.*	<i>b</i> (Å)	St. dev.*	<i>c</i> (Å)	St. dev.*	$\beta$ (°)	St. dev.*	V(Å <sup>3</sup> )	St. dev.*	Crystal mosaicity
300	9.8177	0.001	25.6597	0.0031	19.3047	0.0023	104.384	0.004	4710.78	0.09	0.39
280	9.8071	0.0002	25.6011	0.0007	19.2577	0.0005	104.347	0.001	4684.29	0.02	0.38
260	9.7994	0.0002	25.5488	0.0007	19.2173	0.0005	104.313	0.001	4661.95	0.02	0.38
240	9.7912	0.0002	25.4967	0.0008	19.1789	0.0005	104.291	0.001	4639.72	0.02	0.38
220	9.7836	0.0002	25.4438	0.0008	19.1399	0.0006	104.278	0.001	4617.36	0.02	0.38
200	9.7770	0.0003	25.3964	0.001	19.1058	0.0007	104.272	0.001	4597.56	0.03	0.38
180	9.7754	0.0003	25.3489	0.0008	19.0721	0.0006	104.284	0.001	4579.88	0.02	0.38
160	9.7703	0.0003	25.2982	0.0008	19.0409	0.0006	104.279	0.001	4560.96	0.02	0.38
140	9.7661	0.0003	25.2392	0.0008	19.0103	0.0006	104.270	0.001	4541.16	0.02	0.38
120	9.7650	0.0003	25.1863	0.0009	18.9850	0.0007	104.254	0.001	4525.50	0.03	0.38
100	9.7654	0.0004	25.1269	0.0011	18.9626	0.0008	104.199	0.001	4510.75	0.03	0.38

\*Standard deviation calculated from unit cell refinement using the Apex III software suite.

#### 4) Powder X-ray diffraction measurements

Powder X-ray diffraction data were collected using a Bruker D2 PHASER equipped with Lynxeye 1D detector and Ni-filtered Cu K $\alpha$  radiation ( $\lambda = 1.5418 \text{ \AA}$ ; 30 kV, 10 mA generator parameters; restricted by a 1.0 mm divergence slit and a 2.5 Soller collimator). The high resolution PXRD pattern was recorded using Cu K $\alpha$  radiation ( $\lambda = 1.5418 \text{ \AA}$ , 40 kV and 30 mA) on a PANalytical X'pert PRO instrument operating in Bragg-Brentano geometry. Samples were placed in sealed glass capillaries and analysed at room temperature.

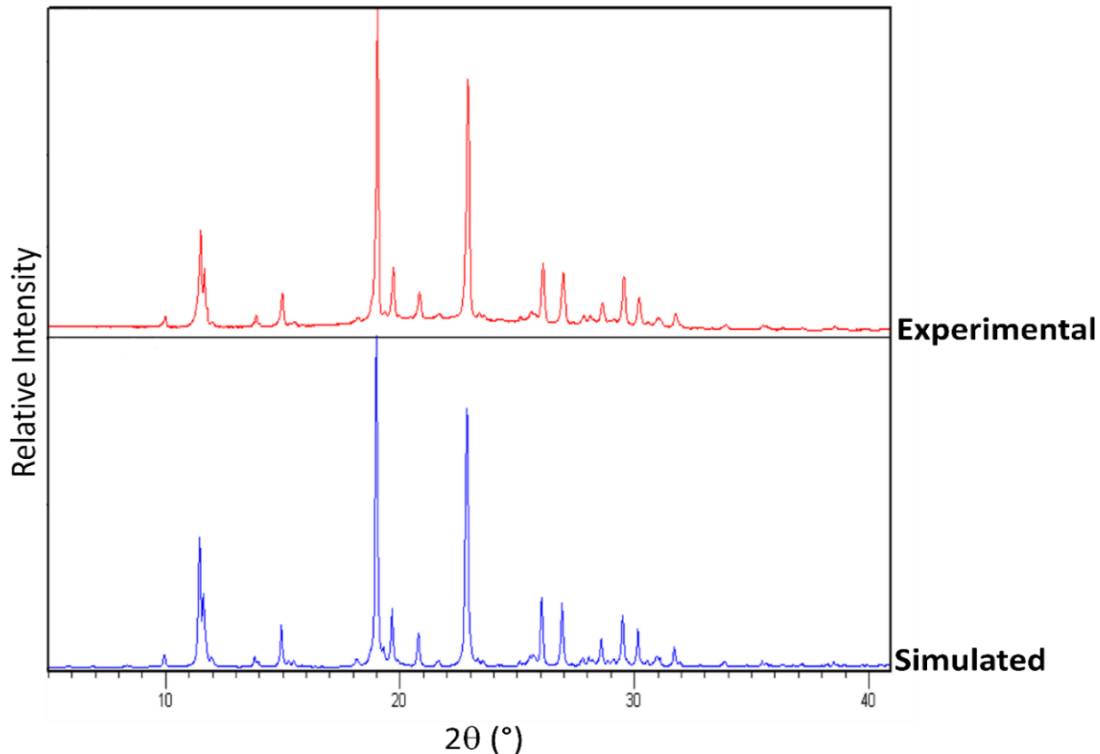


**Figure S1:** PXRD patterns of the experimental and simulated **ABN·2DMABN** cocrystal.

#### 5) Hot stage microscopy

A Linkam DSC600 temperature-controlled hot stage equipped with a digital video camera and LNP95 liquid nitrogen cooling pump was used to record temperature-dependent changes in the appearance of cocrystal **ABN·2DMABN**. The stage was operated via a T95-System Controller. The temperature was ramped from 300 to 100 K and back to 300 K at a ramp rate of  $5 \text{ K min}^{-1}$ .

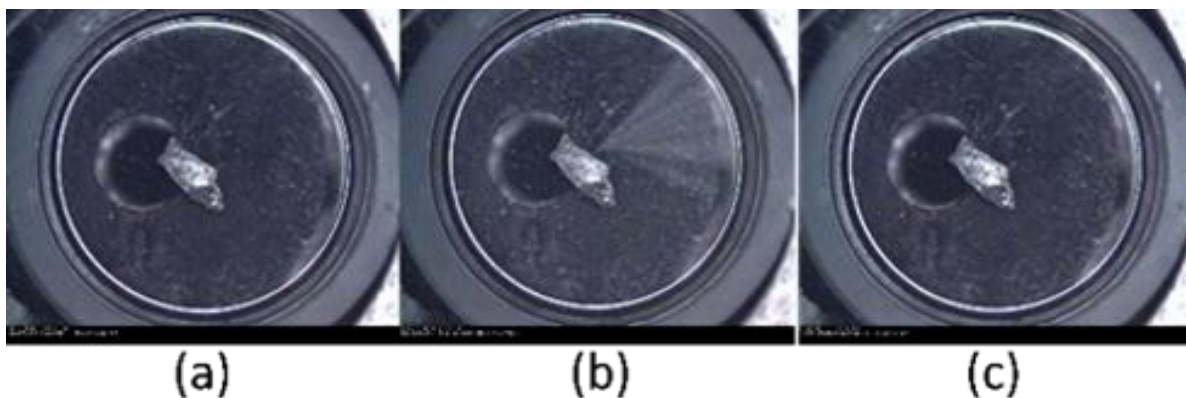


**Figure S2:** The micrographs of **ABN·2DMABN** at a) 300 K cooled to b) 100 K and reheated to c) 300 K.

#### 6) Differential Scanning Calorimetry

Differential scanning calorimetry of **ABN·2DMABN** was carried out on TA DSC-Q100 instrument. Crystals were taken on a Tzero aluminium pan and connected to LNG cryostat for low temperature analysis. The low temperature DSC analysis was carried out by cooling from 300 to 100 K and heated back to 300 K at the heating rate of  $5 \text{ K min}^{-1}$ . Also, the crystal was analysed by heating from room temperature (300 K) to the selected temperature at rate of  $5 \text{ K min}^{-1}$ .

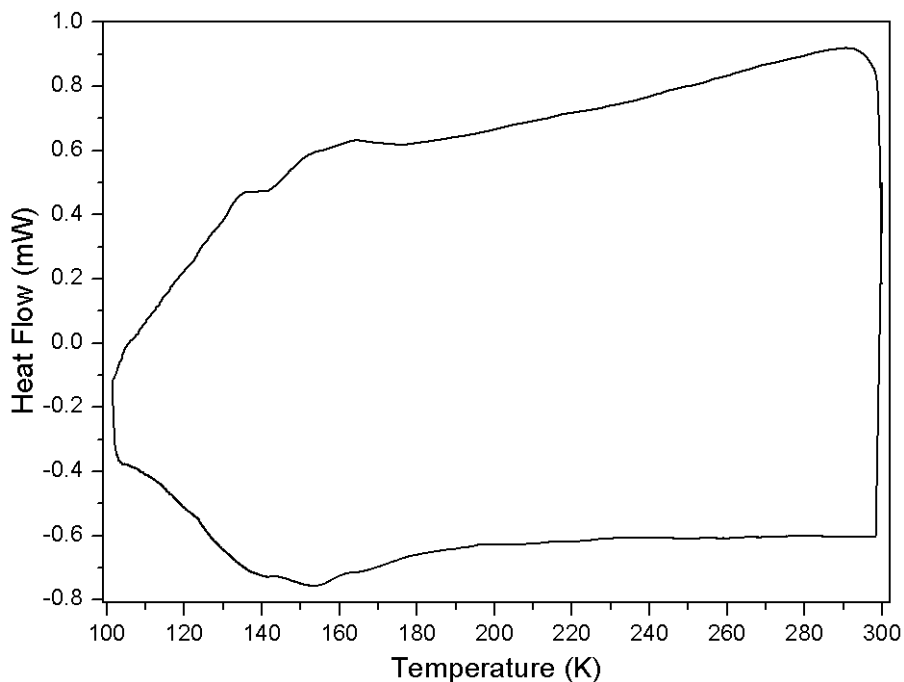


**Figure S3:** The DSC thermogram of the cocrystal **ABN·2DMABN** for the range 100 to 300 K showing no thermal events (no phase change).

## 7) Thermal expansion coefficients

**Table S3.** Linear and volumetric thermal expansion coefficients for **ABN·2DMABN** over different temperature ranges.

Temperature Range (K)	$\alpha_{x1} (\text{MK}^{-1})$	$\alpha_{x2} (\text{MK}^{-1})$	$\alpha_{x3} (\text{MK}^{-1})$	$\alpha_v (\text{MK}^{-1})$
100 – 120	-17.66	62.55	118.34	163.14
120 – 140	2.07	66.69	105.13	173.88
140 – 160	19.30	80.76	117.02	217.13
160 – 180	24.57	82.42	100.31	207.38
180 – 200	7.89	91.40	93.78	193.10
200 – 220	32.09	89.66	93.41	215.27
220 – 240	35.88	102.07	104.06	242.15
240 – 260	36.91	100.29	102.27	239.61
260 – 280	31.15	102.46	105.79	239.52
280 – 300	45.06	114.58	122.90	282.74

**Table S4.** Linear and volumetric thermal expansion coefficients for **ABN·2DMABN** over different temperature ranges that include 300 K.

Temperature Range (K)	$\alpha_{x1} (\text{MK}^{-1})$	$\alpha_{x2} (\text{MK}^{-1})$	$\alpha_{x3} (\text{MK}^{-1})$	$\alpha_v (\text{MK}^{-1})$
100 – 300	24.26	90.88	105.01	222.01
120 – 300	27.13	94.22	103.68	226.72
140 – 300	29.53	96.91	102.90	230.93
160 – 300	31.33	99.08	101.93	233.93
180 – 300	33.46	101.42	102.54	238.85
200 – 300	36.26	103.84	104.41	245.61
220 – 300	36.90	105.89	107.21	250.91
240 – 300	37.16	106.69	109.49	254.28
260 – 300	38.14	108.75	114.60	262.44
280 – 300	45.06	114.58	122.90	282.74

8) Intermolecular interactions in the structure

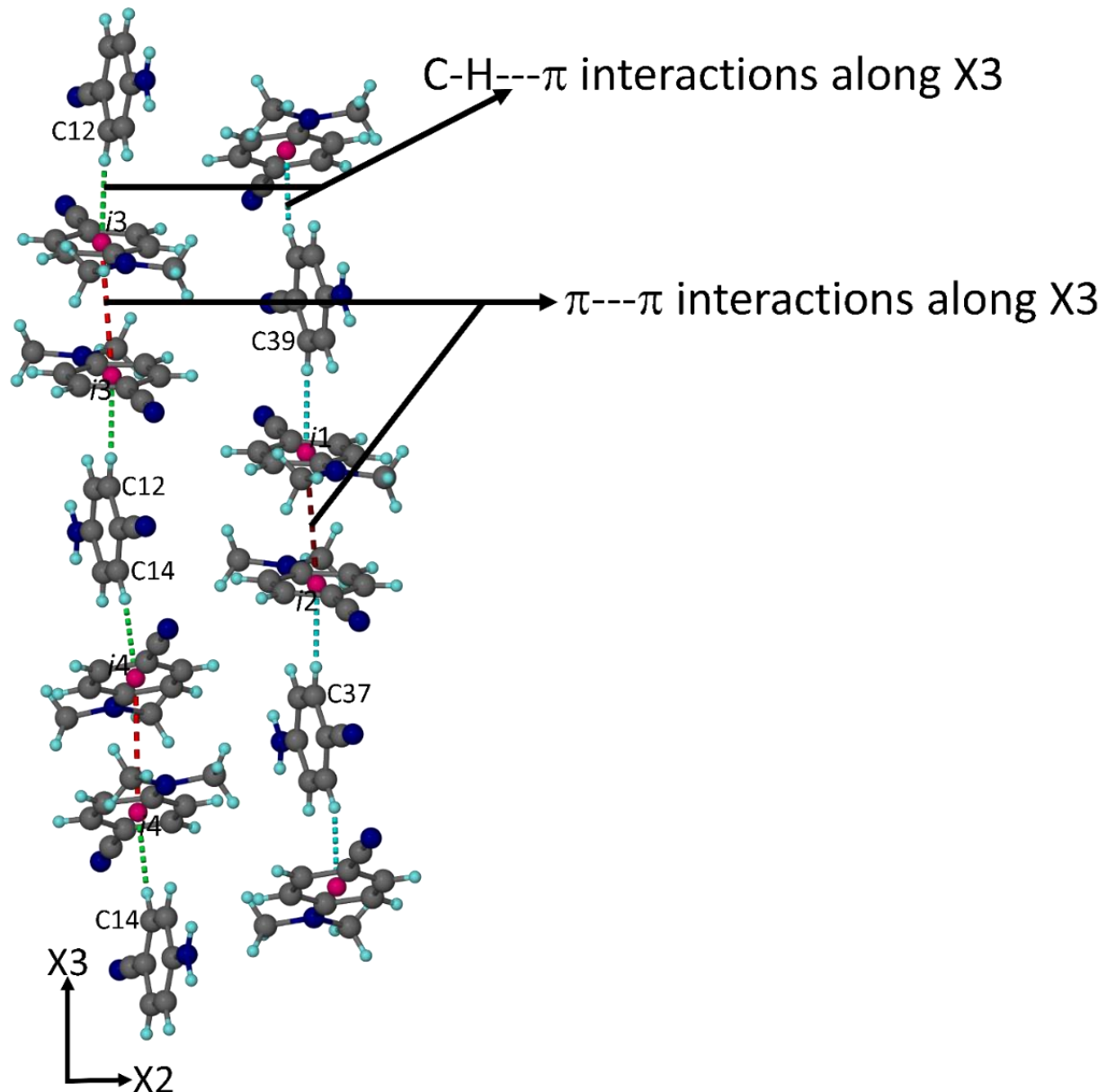


**Figure S4:** Perspective view showing C-H $\cdots$  $\pi$  and  $\pi\cdots\pi$  interactions along the principal axis X3.

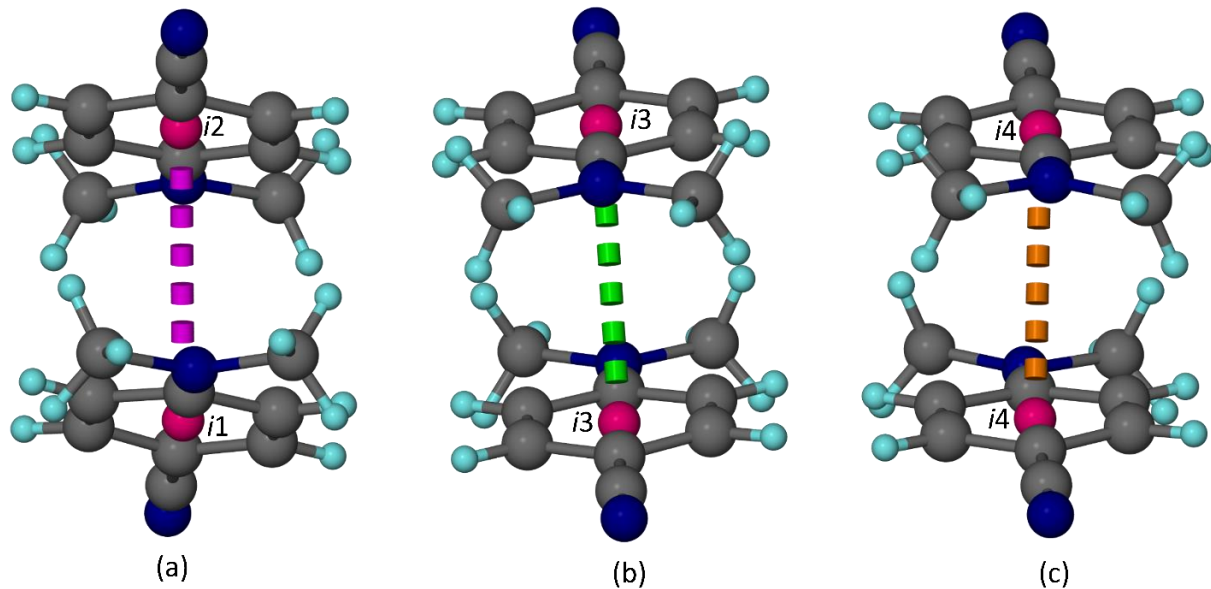


**Figure S5:** Views showing all the centroid-to-centroid distances ( $\text{\AA}$ ) along the principal axis X3 with (a)  $i_1$ --- $i_2$  (b)  $i_3$ --- $i_3$  and (c)  $i_4$ --- $i_4$ .  $i_1$  is the centroid of C26-C31,  $i_2$  is the centroid of C42-C47,  $i_3$  is the centroid of C1-C6 and  $i_4$  is the centroid of C17-C22.

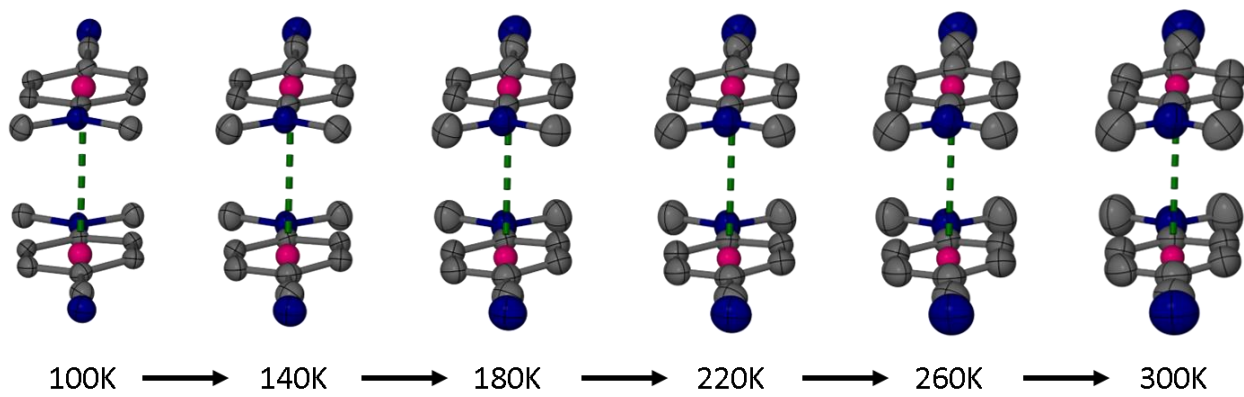


**Figure S6:** Views showing the increase in ellipsoids as the temperature increases along the principal axis X3 (30% probability).

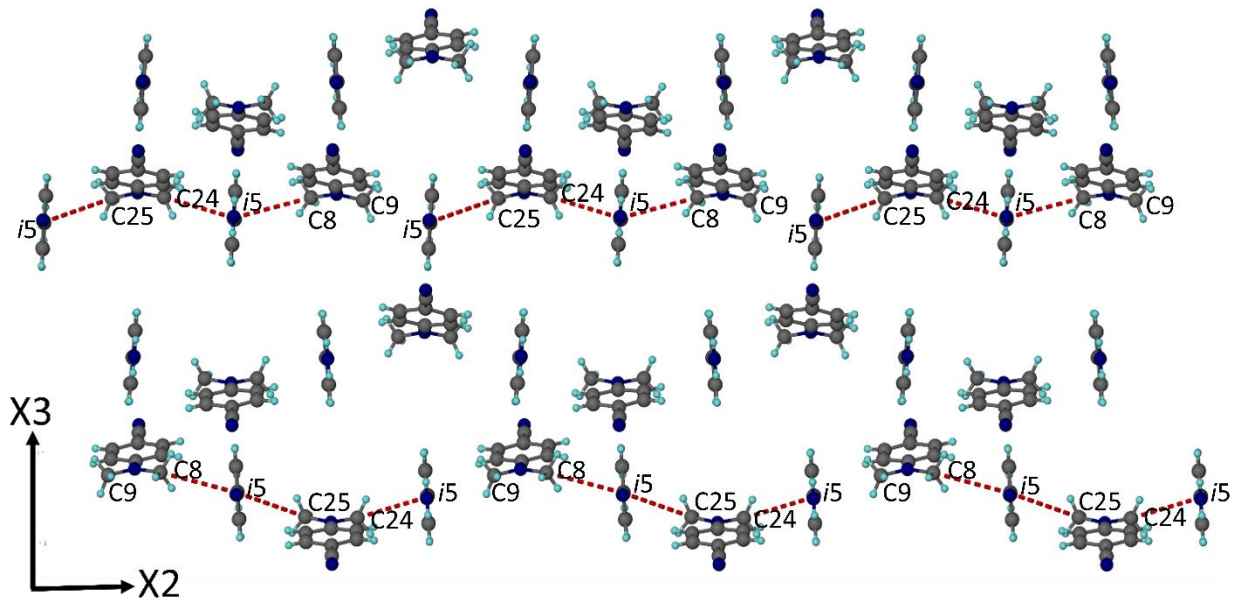


**Figure S7:** Perspective view showing C-H $\cdots\pi$  interactions along the principal axis X2.

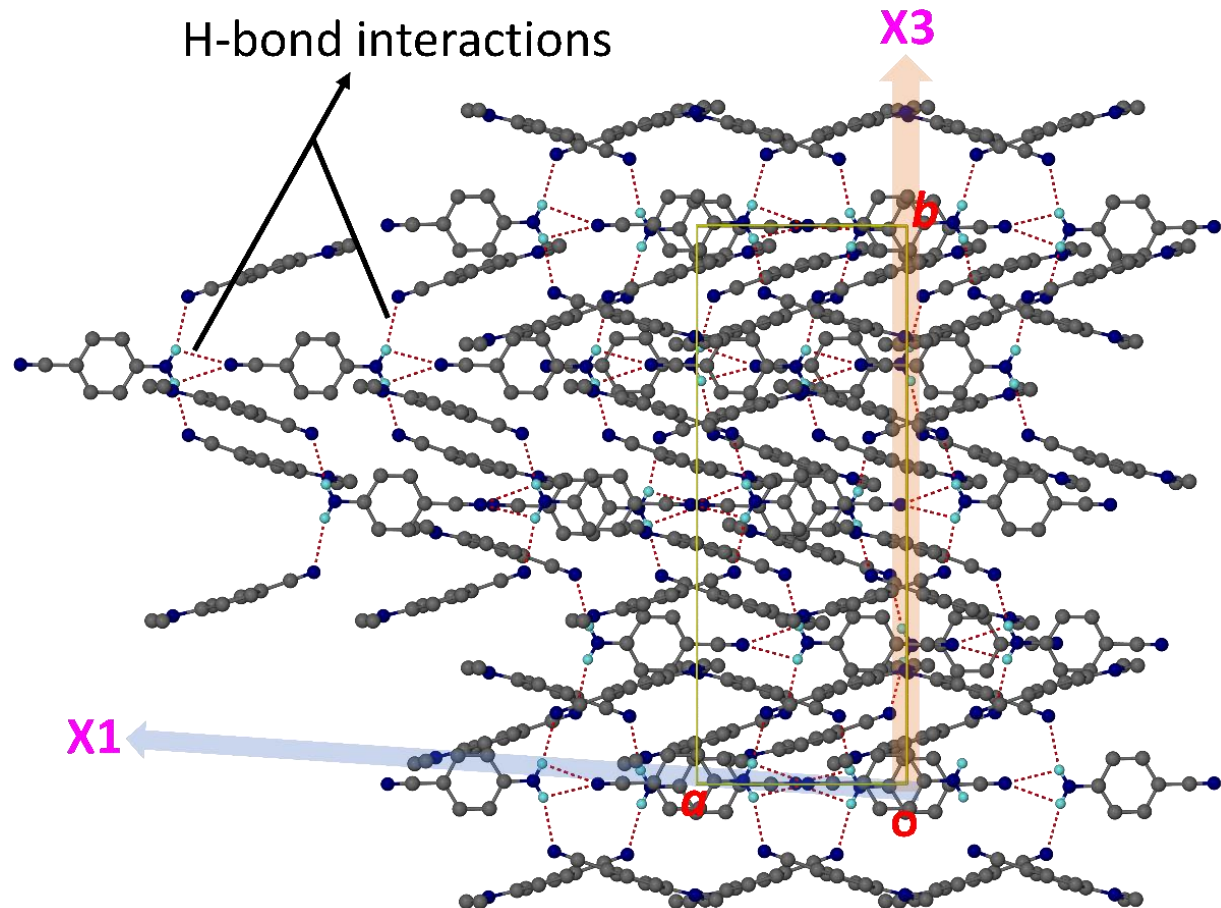


**Figure S8:** Perspective view of the ABN·2DMABN cocrystal showing N-H $\cdots$ N hydrogen bonding interactions along the principal axis X1.

The program PLATON was used to generate a list of hydrogen bond distances ( $D \cdots A$ ) ( $\text{\AA}$ ) in the **ABN·2DMABN** cocrystal from 100 to 300 K.

**Table S5.** Some intermolecular interaction distances ( $\text{\AA}$ ) within the molecules at different temperatures for **ABN·2DMABN** cocrystal along the principal axis X3.

Distance ( $\text{\AA}$ )	T (K)										RC
	100	120	140	160	180	200	220	240	260	280	
$\pi \cdots \pi$ ( $i1 \cdots i2$ )	3.8843(2)	3.9064(1)	3.9241(1)	3.9293(1)	3.9536(1)	3.9615(2)	3.9704(1)	3.9819(1)	3.9910(1)	4.0021(1)	4.0134(5)
$\pi \cdots \pi$ ( $i3 \cdots i3$ )	3.9594(2)	3.9801(1)	3.9960(1)	4.0109(1)	4.0209(1)	4.0286(2)	4.0384(1)	4.0472 (1)	4.0526(1)	4.0612(1)	4.0724(5)
$\pi \cdots \pi$ ( $i4 \cdots i4$ )	3.8275(2)	3.8488(1)	3.8679(1)	3.8845(1)	3.8948(1)	3.9062(2)	3.9156(1)	3.9261(1)	3.9360(1)	3.9360(1)	3.9565(5)
<b>C12-H12<math>\cdots</math><math>\pi</math></b> <b>(C12<math>\cdots</math>i3)</b>	3.4874(1)	3.4948(1)	3.5032(1)	3.5130(1)	3.5247(1)	3.5329(1)	3.5429(1)	3.5575(1)	3.5710(1)	3.5847(1)	3.5969(4)
<b>C14-H14<math>\cdots</math><math>\pi</math></b> <b>(C14<math>\cdots</math>i4)</b>	3.4770(1)	3.4852(1)	3.4983(1)	3.5091(1)	3.5226(1)	3.5298(1)	3.5425(1)	3.5543(1)	3.5679(1)	3.5809(1)	3.5956(4)
<b>C37-H37<math>\cdots</math><math>\pi</math></b> <b>(C37<math>\cdots</math>i2)</b>	3.5245(1)	3.5307(1)	3.5404(1)	3.5500(1)	3.5649(1)	3.5688(1)	3.5813(1)	3.5917(1)	3.6064(1)	3.6202(1)	3.6324(4)
<b>C39-H39<math>\cdots</math><math>\pi</math></b> <b>(C39<math>\cdots</math>i1)</b>	3.4453(1)	3.4530(1)	3.4644 (1)	3.4760(1)	3.4870(1)	3.4989(1)	3.5097(1)	3.5228(1)	3.5351(1)	3.5463(1)	3.5619(4)

$i1$ = centroid of C26-C31,  $i2$ = centroid of C42-C47,  $i3$ = centroid of C1-C6 and  $i4$ = centroid of C17-C22.

RC= Relative change with respect to 100 K.

**Table S6.** Some important C-H $\cdots$  $\pi$  interactions within the molecules at different temperatures for **ABN·2DMABN** cocrystal along X2.

Distance ( $\text{\AA}$ )	T (K)										RC
	100	120	140	160	180	200	220	240	260	280	
<b>C8-H8C<math>\cdots</math><math>\pi</math></b> <b>(C8<math>\cdots</math>i5)</b>	4.0048(1)	3.9943(1)	3.9899(1)	3.9897(1)	3.9966(1)	4.0138(1)	4.0259(1)	4.0425(1)	4.0587(1)	4.0707(1)	4.0872(4)
<b>C24-H24C<math>\cdots</math><math>\pi</math></b> <b>(C24<math>\cdots</math>i5)</b>	3.6578(1)	3.6650(1)	3.6738(1)	3.6845(1)	3.6908(1)	3.6948(1)	3.7015(1)	3.7064(1)	3.7111(1)	3.7171(1)	3.7243(4)
<b>C25-H25B<math>\cdots</math><math>\pi</math></b> <b>(C25<math>\cdots</math>i5)</b>	4.1145(1)	4.1292(1)	4.1453(1)	4.1590(1)	4.1766(1)	4.1904(1)	4.2075(1)	4.2266(1)	4.2455(1)	4.2657(1)	4.2837(4)

$i5$ = centroid of C35-C40.

RC= Relative change with respect to 100 K.

**Table S7.** Hydrogen bond parameter, D (distance ( $\text{\AA}$ ) between H-bond donor and H-bond acceptor) at different temperatures for **ABN·2DMABN** cocrystal along X1.

D…A ( $\text{\AA}$ )	T (K)										
	100	120	140	160	180	200	220	240	260	280	300
<b>N3-H3D…N6</b>	3.275(3)	3.274(4)	3.275(4)	3.278(4)	3.286(4)	3.288(4)	3.296(3)	3.301(4)	3.304(4)	3.316(4)	3.326(5)
<b>N3-H3E…N2</b>	3.334(3)	3.343(4)	3.341(4)	3.346(4)	3.350(4)	3.350(4)	3.352(3)	3.356(4)	3.359(4)	3.362(4)	3.358(5)
<b>N9-H9E…N8</b>	3.259(4)	3.264(4)	3.267(4)	3.268(4)	3.276(4)	3.284(4)	3.287(3)	3.297(4)	3.310(4)	3.309(4)	3.323(5)
<b>N9-H9D…N12</b>	3.344(4)	3.340(4)	3.345(4)	3.344(4)	3.346(4)	3.346(4)	3.350(3)	3.351(3)	3.360(4)	3.362(4)	3.370(5)

**Table S8.** Hydrogen bond parameter showing bond angle ( $^{\circ}$ ) between H-bond donor and H-bond acceptor at different temperatures for **ABN·2DMABN** cocrystal along X1.

>D-H…A ( $^{\circ}$ )	T (K)										
	100	120	140	160	180	200	220	240	260	280	300
<b>N3-H3D…N6</b>	166.77(17)	167.16(18)	166.74(20)	166.71(21)	166.41(21)	166.30(17)	166.01(19)	166.15(19)	166.71(21)	165.87(23)	166.14(24)
<b>N3-H3E…N4</b>	161.65(17)	161.66(18)	161.75(19)	161.88(21)	161.93(21)	161.90(17)	162.09(19)	161.97(19)	161.56(20)	161.98(23)	161.91(24)
<b>N9-H9E…N8</b>	168.33(17)	168.09(18)	168.02(20)	167.68(21)	167.32(21)	167.45(17)	167.24(19)	166.96(19)	166.13(20)	166.67(22)	165.80(26)
<b>N9-H9D…N12</b>	160.22(17)	160.23(18)	160.70(19)	160.86(21)	161.15(21)	161.02(17)	161.27(19)	161.42(19)	162.00(20)	161.47(22)	161.74(26)

**Table S9.** Showing bond distance ( $\text{\AA}$ ) between H-donor Nitrogen and H-acceptor Nitrogen at different temperature for **ABN·2DMABN** cocrystal along the principal axis X1.

Distance ( $\text{\AA}$ )	T (K)										RC
	100	120	140	160	180	200	220	240	260	280	
<b>N3…N4</b>	3.0106(1)	3.0192(1)	3.0207(1)	3.0295(1)	3.0376(1)	3.0459(1)	3.0533(1)	3.0639(1)	3.0739(1)	3.0853(1)	3.0990 (3)
<b>N9…N10</b>	3.0171(1)	3.0174(1)	3.0217(1)	3.0281(1)	3.0342(1)	3.0434(1)	3.0528(1)	3.0627(1)	3.0717(1)	3.0834(1)	3.0931 (3)

RC= Relative change with respect to 100 K.

## References

1. SAINT Data Reduction Software, Version 6.45; Bruker AXS Inc.: Madison, WI, 2003.
2. SADABS, Version 2.05; Bruker AXS Inc.: Madison, WI, 2002.
3. R. H. Blessing, An Empirical Correction for Absorption Anisotropy. *Acta Crystallogr., Sect. A: Found. Crystallogr.* 1995, **51**, 33–38.
4. G. M. Sheldrick, A Short History of SHELX. *Acta Crystallogr., Sect. A: Found. Crystallogr.* 2008, **64**, 112.

5. L. Barbour, X-Seed – A Software Tool for Supramolecular Crystallography. *J. Supramol. Chem.* 2001, **1**, 189.